



Article

Eccentricity in Induction Machines—A Useful Tool for Assessing Its Level

Janusz Petryna ¹, Arkadiusz Duda ² and Maciej Sułowicz ^{2,*}

¹ Department of Electrical Engineering, Polytechnic Faculty, University of Applied Sciences in Tarnow, Mickiewicza 8 Str., 33-100 Tarnow, Poland; j_petryna@pwszta.edu.pl

² Department of Electrical Engineering, Faculty of Electrical and Computer Engineering, Cracow University of Technology, Warszawska 24 Str., 31-155 Cracow, Poland; arkadiusz.duda@pk.edu.pl

* Correspondence: maciej.sulowicz@pk.edu.pl; Tel.: +481-2628-2658

Abstract: In the condition monitoring of induction machines operating in various industry sectors, the assessment of eccentricity is as important as the assessment of the condition of windings, bearings, mechanical vibrations or noise. The reasons for the eccentricity can be various; for example, rotor imbalance, damage or wear of the bearings, improper alignment of the rotor and the load machine and finally, assembly errors after overhaul. Disregard of this phenomenon during routine tests may result in the development of vibrations transmitted to the stator windings, faster wear of the bearings and even, in extreme cases, rubbing of the rotor against the stator surface and damage to the windings and local overheating of the machine core. On the basis of years of experience in the diagnosis of large induction machines operating in various industries, the article deals with the problem of developing reliable indicators for assessing the levels of commonly accepted types of eccentricity. Starting from field calculations and analyzing various cases of eccentricity, the methodology for determining the indicators for evaluation from the stator current spectrum is shown. The changes in the values of these indices for various cases of simultaneous occurrence of static and dynamic eccentricity are shown. The calculation results were verified in the laboratory. Also shown are three interesting cases from diagnostic practice in the evaluation of high-power machines in the industry. It has been shown that the proposed indicators are useful and enable an accurate diagnosis of levels of eccentricity.

Keywords: induction motor; diagnostic indicators; eccentricity; industry; condition monitoring; diagnostics of eccentricity; numerical coefficients; current; axial flux; spectrum; monitoring; trend



Citation: Petryna, J.; Duda, A.; Sułowicz, M. Eccentricity in Induction Machines—A Useful Tool for Assessing Its Level. *Energies* **2021**, *14*, 1976. <https://doi.org/10.3390/en14071976>

Academic Editors: Chunhua Liu and Sheldon Williamson

Received: 5 February 2021

Accepted: 31 March 2021

Published: 2 April 2021

Publisher's Note: MDPI stays neutral with regard to jurisdictional claims in published maps and institutional affiliations.



Copyright: © 2021 by the authors. Licensee MDPI, Basel, Switzerland. This article is an open access article distributed under the terms and conditions of the Creative Commons Attribution (CC BY) license (<https://creativecommons.org/licenses/by/4.0/>).

1. Introduction

Reliable diagnostics of induction machines, in addition to recognizing the continuity and symmetry of windings, the condition of the iron packet and the mechanical condition, cannot do without assessing the level of eccentricity [1–8]. The work [1] and the work of the authors [2–6] show how to extract characteristic features from the current spectrum to determine diagnostic indicators in a practical way.

Measurements of mechanical vibrations around the bearings or machine body often indicate their increase, which is most often associated with the condition of the bearings, unstable foundation or misalignment of the motor and working machine, which is usually true, but this is usually the result and not the cause.

The reason for the increase in vibration and noise may be just eccentricity, which affects the operation and condition of the entire machine, including vibration of the coils in the slots, faster wear or even damage to the bearings, and can even cause the worst problem of rotor to stator rubbing with all its consequences.

Therefore, it is worth introducing, as in the case of vibrations, a numerical description of the phenomenon that will allow tracking its development over time, as well as the possibility of comparing different machines according to one single criterion.

The concept of introducing numerical indicators for the description of the degree of eccentricity is justified by the authors due to positive experiences with the similar description of the winding condition of an induction motor rotor by means of Rotor Fault Index (RFI) [9,10]. They are also calculated on the basis of so-called slip harmonic amplitudes in the stator current or axial flux spectrum. The range of their variability corresponds to the degree of degradation of the rotor windings from early high resistance joints up to the number of broken bars or broken end rings in the rotor cage. Based on subsequent measurements, it is possible to determine the trend, the period of further safe operation if still possible and the date of the next test. Thanks to this, the owner of the installation or the maintenance engineer is not surprised by the sudden shutdown of the machine due to a failure, but can schedule the shutdown and repair of the machine at the appropriate time. In a complete machine condition analysis, data on changes in eccentricity from measurement to measurement are as important as data on cage health, vibration, noise and temperature.

The most frequently used signal for diagnosing rotor eccentricity is the stator current [8,11–15]. This method consists of finding harmonics in the current spectrum with frequencies characteristic for a given type of eccentricity and then analyzing their amplitudes. For the diagnosis of eccentricity, the zero-sequence current [16–18] can also be used in the case of a delta connection of the windings or the zero-sequence voltage [19] in the case of star-connected windings. The formulas on characteristic frequencies of these two methods take into account the saturation effect of the magnetic core of the motor, which strongly affects the zero-sequence component of current and voltage. In order to detect motor eccentricity, the machine's electromagnetic flux can be used.

Articles [5,20–23] describe the use of spectral analysis of the stray flux or the magnetic field of the motor. As with the current method, flux-based diagnostics consist of searching for harmonics and measuring their amplitudes.

The aforementioned articles accurately describe the effects in the form of various signals caused by the eccentric rotor operation. When there is a need to quantify the level of eccentricity, which from the authors' experience may vary depending on the type and size of the machine, the problem begins to arise. This article presents proposals for eccentricity (static, dynamic and mixed) indicators that have been tested with the Finite Elements Method calculations (FEM), laboratory and industrial measurements over several years.

With a modern approach to diagnosing faults in electrical machines and proper forecasting of repair activities, it is important to use new methods of condition assessment, including diagnostic methods based on artificial and computational intelligence [24,25].

The rest of the paper is organized as follows: in the second section, the eccentricity, its types and negative effects are discussed. The definition of indicators used by the authors to evaluate machines in the industry is also given here. The third section contains a description of the FEM model of the machine, which was used to illustrate how to derive indicators for determining levels of eccentricity.

In Section 4, the results of laboratory measurements and determining an indicator to evaluate the levels of eccentricity are presented.

Section 5 provides examples of the use of indicators to assess the condition of industrial motors. These motors work in important technological installations, for which during several years of practice these indicators have been effectively used to assess the levels of eccentricity. In Section 6, the discussions of the results are presented. Finally, conclusions are given in Section 7.

2. Types of Eccentricity and Assessment Indicators as Comparative Criteria

Taking into account the eccentricity in the mathematical model of the machine is related to the air gap permeance function, which in turn depends on the changes in the length of the air gap. Such a function depends on the angular coordinate of the stator and the angle of rotation of the rotor. In publications [26,27], various forms of the permeance function depending on the type of eccentricity were presented. This chapter mainly focuses on the prac-

tical aspects of identifying types of eccentricity and their negative impact on the design of the machine.

2.1. Static Eccentricity

The reason for static eccentricity may be incorrect assembly of the machine or significant wear of the bearings. The shape of the air gap between the stator and the rotor along the circumference of the stator remains unchanged both at standstill and during machine operation. It is shown in Figure 1.

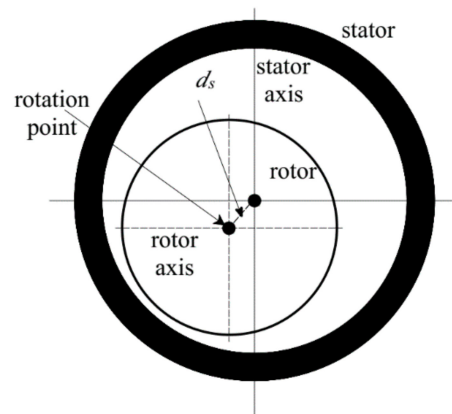


Figure 1. Static eccentricity of the rotor.

Adverse phenomena that can be caused by significant static eccentricity are:

- shaft torque drops according to the Formula [3]:

$$T_b = T_{bn} \left(1 - \varepsilon_s^2\right)^{\frac{1}{2}}, \quad (1)$$

where: T_b —critical (maximum) torque, T_{bn} —critical nominal torque, ε_s —relative value of the static eccentricity factor,

- unbalanced magnetic tension forces with radial and tangential components:

The radial component causes vibrations to be transmitted to the bearings, while the tangential component does not reveal to the outside but is closed inside the bearing, causing its wear and tear, i.e., significant looseness, which in turn causes radial vibrations.

In this case, static eccentricity is the primary cause of dynamic eccentricity. Both of those phenomena can overlap.

The level of static eccentricity is calculated from [27]:

$$\varepsilon_s = \frac{d_s}{\delta_0}, \quad (2)$$

where δ_0 is an average air gap length considering the slot opening geometry and the Carter's factor of a healthy motor.

The frequencies of the spectrum components specific to static eccentricity belong to the set described by the formula [1,2,6]:

$$f_{stat} \in \left\{ \frac{kNn}{60} \pm lf_0 \right\} \setminus \{f_{sym}\}, \quad (3)$$

where: $k = 1, 2, 3, \dots$, $l = 1, 3, 5, \dots$, N —number of rotor slots, n —rotor speed, p —number of pole pairs, f_0 —mains voltage frequency, k can be 1, 2, 3 and many next values, depending on the spectrum features.

The components present in the motor current spectrum are always [1,2,6]:

$$f_{sym} \in \left\{ \frac{kgNn}{60} \pm lf_0 \right\} \quad (4)$$

where $g = \{1, 2, \dots, 2p\}$. The product of gN belongs to: $\{6kp\}$ or $\{6kp + 2p\}$ or $\{6kp + 4p\}$. These components are typical for the electrical and magnetic symmetry of the machine. Typical k values are 1, 2, 3, but some next values are also possible; it depends on the amount of spectrum components, including amount of PSHs (principal slot harmonics) related to the number of supply harmonics and range of spectrum frequency recorded; however, their amplitudes get smaller or do not exceed the noise level.

2.2. Dynamic Eccentricity

During machine operation, the minimum width of the air gap moves along the stator circumference. It is shown in Figure 2. The sources of dynamic eccentricity can be:

- shaft deflection and unbalance,
- mechanical resonance at critical revolutions,
- bearing wear.

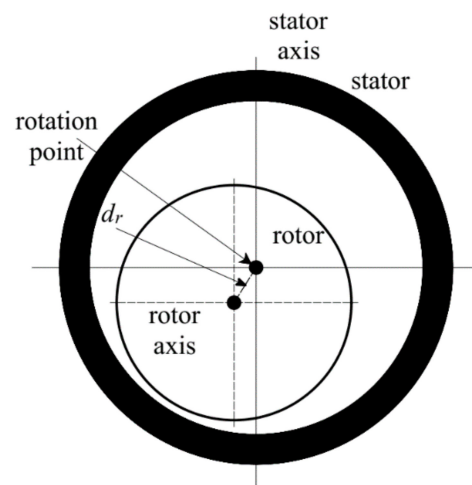


Figure 2. Dynamic eccentricity of the rotor.

Adverse phenomena that can be caused by significant dynamic eccentricity are:

- increase in vibration due to uneven magnetic tension,
- possible rotor friction on the stator-stalling, sparking, damage to the core packet sheets, increased iron losses, decrease in efficiency,
- vibrations (of the order of kHz) transmitted to the stator, causing mechanical damage to the insulation,
- induced voltages at shaft ends leading to a reduction in bearing life,
- dislocation, damage or premature wear of bearings,
- increased motor start time.

The level of dynamic eccentricity is calculated from [27]:

$$\varepsilon_d = \frac{d_r}{\delta_0}. \quad (5)$$

The frequencies of the spectrum components specific to dynamic eccentricity belong to the set [1,2,6]:

$$f_{dyn} \in \left\{ \frac{k2pn}{60} \pm lf_0 \right\} \setminus (\{f_{sym}\} \cup \{f_{sta}\}) \quad (6)$$

2.3. Mixed Eccentricity

Mixed eccentricity is the result of simultaneous static and dynamic eccentricity, or simultaneous static eccentricity and damage to the cage. It is accompanied by bearing vibrations and core packet vibrations.

The frequencies of the spectrum components specific for mixed eccentricity belong to the set [1,2,6]:

$$f_{mix} \in \left\{ \frac{kn}{60} \pm lf_0 \right\} \setminus \left(\{f_{sym}\} \cup \{f_{sta}\} \cup \{f_{dyn}\} \right) \quad (7)$$

Due to the above frequency spectra by Formulas (2)–(5), the sets of amplitudes can be obtained on the basis of which the indicators for assessing eccentricity levels can be determined.

2.4. Indicators for Eccentricity Assessment

Based on the spectrum of the current or axial flux expressed in dB or physical units, for any type of eccentricity the indicators for its assessment can be defined.

Two indicators have been defined for the characteristic amplitudes of the spectrum components [2]: Eccentricity Amplitude Level Index (*EALI*)

$$EALI_{Type} = \frac{\sum A_{eccType}}{\sum A_{sym}} \quad (8)$$

and Eccentricity Square Amplitude Level Index (*ESALI*)

$$ESALI_{Type} = \frac{\sum A_{eccType}^2}{\sum A_{sym}^2} \quad (9)$$

where:

- $A_{eccType}$ —harmonic amplitudes for a given type of eccentricity, where *eccType* is a kind of eccentricity: static—*stat*, dynamic—*dyn*, mixed—*mix*.
- A_{sym} —amplitude of the basic slot harmonic (*Psh*) appropriate for magnetic symmetry.

The use of the above indicators will normalize the spectra numerically, assigning a number to each of them, without omitting any authorized component of the given spectrum. Thanks to this, it is possible to determine the eccentricity trend for a given machine, i.e., changes in the level of eccentricity in time, and make a comparison with the levels of mechanical vibrations. Measurement experience indicates a relationship between the eccentricity of the machine and the level of its vibrations. Therefore, the maximum eccentricity is determined for a given motor by the increase of vibrations to its still permissible values (the expression “still permissible” according to standards). This level may be different for different machines.

3. FEM Simulations

3.1. FEM Model

To simulate the two-dimensional field model of the induction motor, the *Ansys Maxwell* computing environment, namely the Maxwell 2D program with the *Transient Solver* add-on, was used.

The *Transient Solver* add-on is responsible for performing field calculations with moving parts. To introduce the geometry of the motor, a special tool dedicated to designing rotating electric machines—*RMxpert* was used.

The object of the field tests was the Sg112M-4 motor with the following data: $P_N = 4$ kW, $U_N = 400$ V, $I_N = 8.1$ A, $n_N = 1430$ rpm, $p = 2$ and the number of stator slots $N_s = 36$ and rotor bars $n = 28$. On the basis of the motor winding card and technical drawings of the stator and rotor, the geometries of the tested motor were introduced, supplemented with the data from the rating plate.

As a result of entering the data into the *RMxpert* program, the motor design was obtained (Figure 3), which was then processed into the *Maxwell 2D* model (Figure 4).

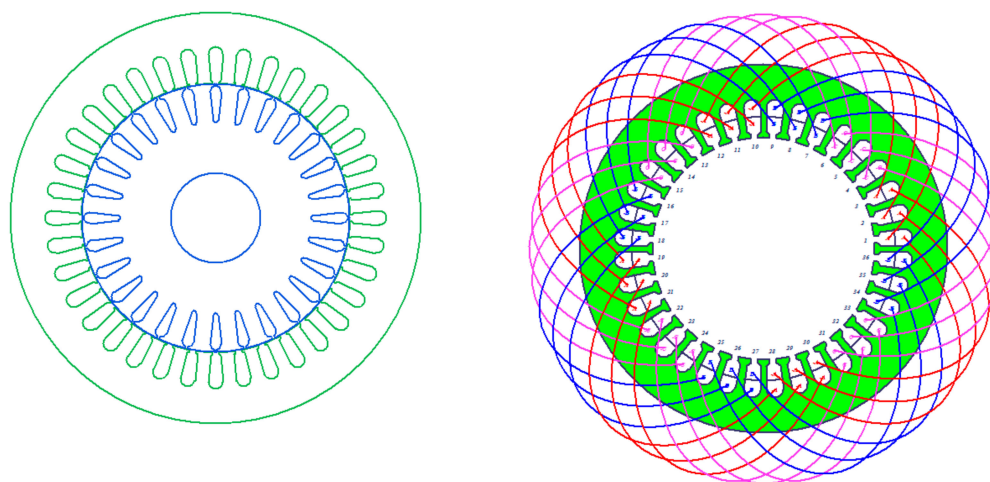


Figure 3. Stator and rotor yoke (from the left); coils connections diagram.

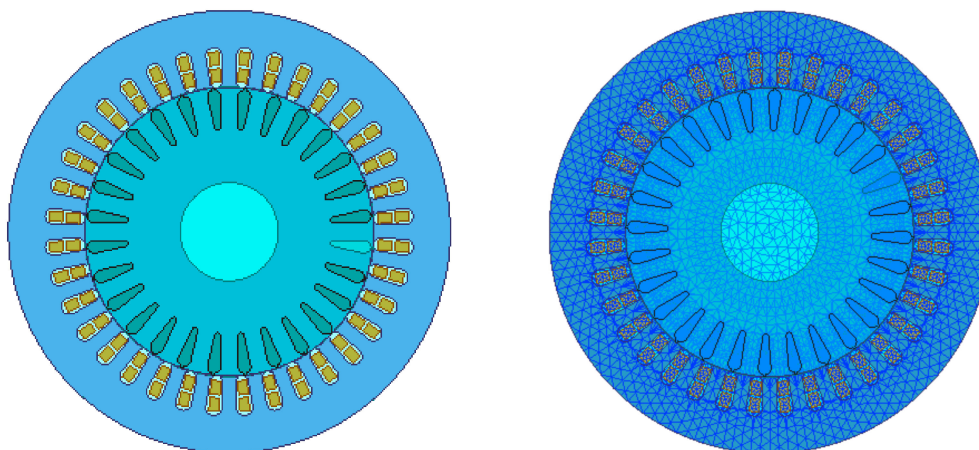


Figure 4. 2D model of the Sg112M-4 motor in Maxwell 2D software and a mesh image (on the right).

The next step was to model the motor damages properly. Due to the division of the eccentricity into three types, which were quoted and described above, some changes of geometry in the positioning of the stator and rotor were made. The air gap in the tested motor is $\delta_0 = 0.3$ mm. The individual types of eccentricity have been modeled according to the definitions in Section 2:

- dynamic eccentricity—shifting the rotor axis by the vector $\langle 0, 0.23 \rangle$ mm, which gives the relative eccentricity: $\varepsilon_d = 0.77$, $\varepsilon_s = 0$; the axes of rotation and symmetry of the stator remain unchanged,
- static eccentricity—shifting the stator axis by the vector $\langle 0, 0.23 \rangle$ mm, which gives the relative eccentricity $\varepsilon_d = 0$, $\varepsilon_s = 0.77$; the axes of rotation and symmetry of the rotor remain unchanged,
- mixed eccentricity—shifting the stator axis by the vector $\langle 0.06, 0 \rangle$ mm and the rotor by a vector $\langle 0, 0.06 \rangle$, which gives a relative eccentricity: $\varepsilon_d = 0.2$, $\varepsilon_s = 0.2$, the axis of rotation remains unchanged.

The motor was powered by a symmetrical voltage source with the frequency $f_s = 50$ Hz and the effective value 230 V. The rotor speed was set at 1450 rpm. Simulations with a duration of 10 s with a step of 0.1 ms were decided.

3.2. Simulation Results

In Figures 5–8, the harmonics identified for symmetry and all three types of eccentricity are marked by colors, i.e., symmetry—blue, static eccentricity—green, dynamic eccentricity—red, mixed eccentricity—purple.

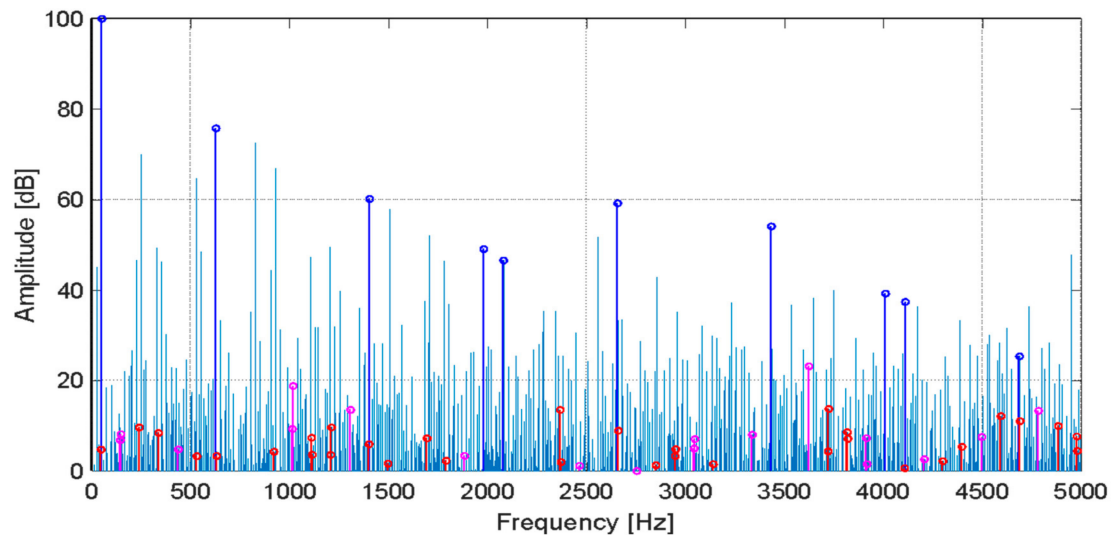


Figure 5. The stator current spectrum for the case of symmetry.

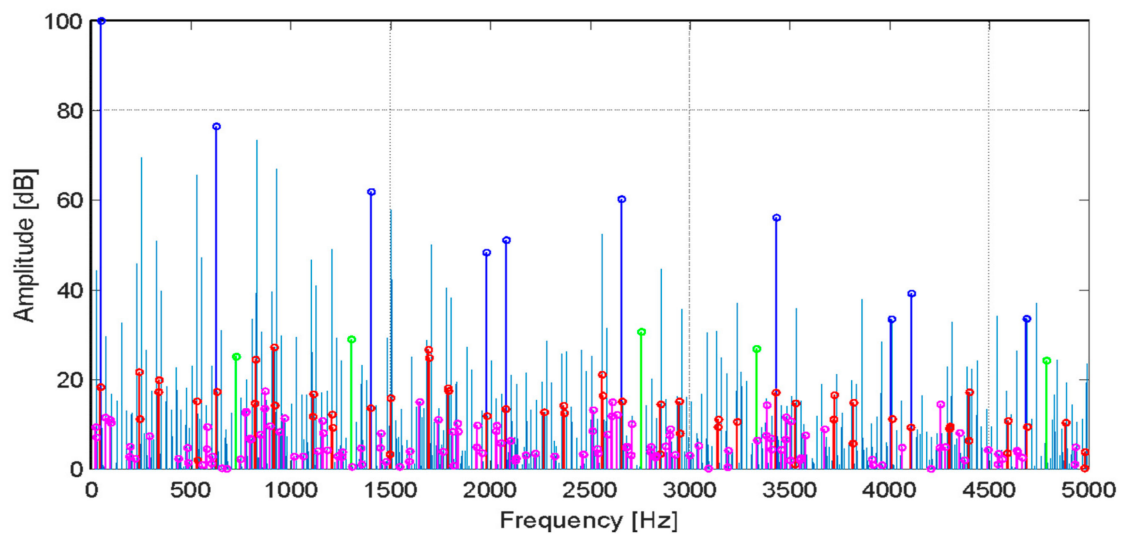


Figure 6. The stator current spectrum for the case of static eccentricity.

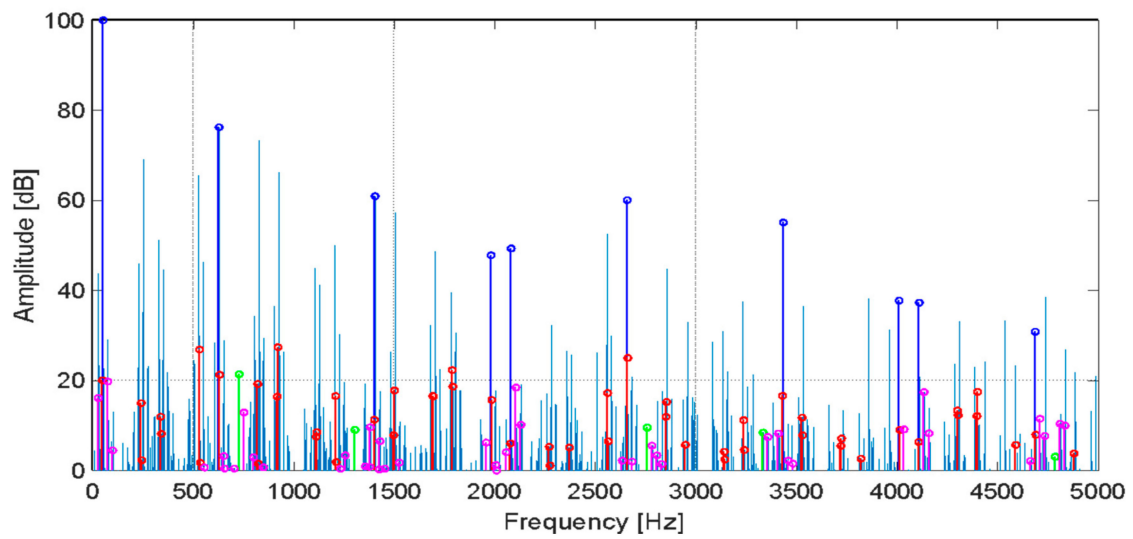


Figure 7. The stator current spectrum for the case of dynamic eccentricity.

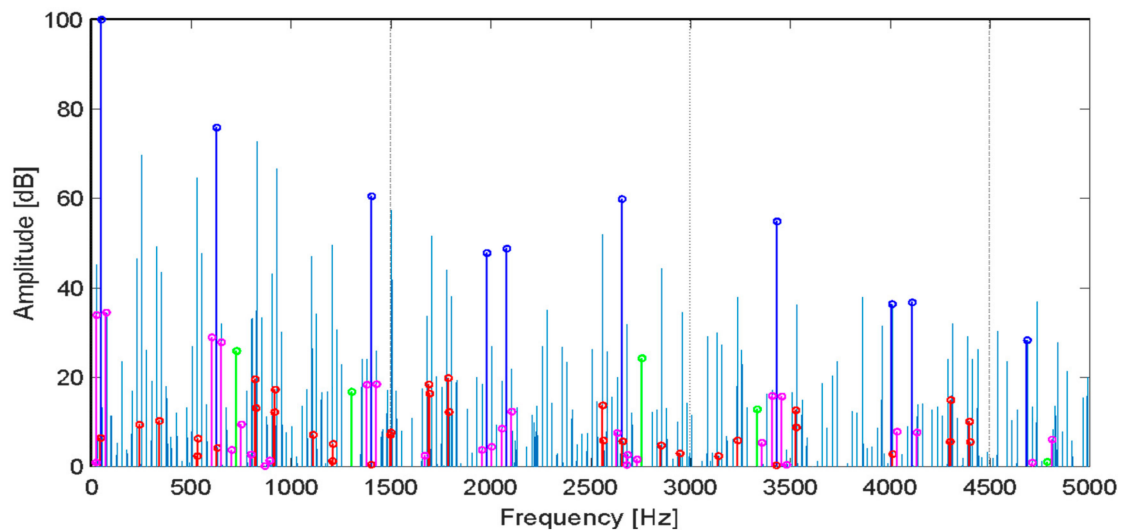


Figure 8. The stator current spectrum for the case of mixed eccentricity.

For example, in Tables 1 and 2 there are harmonic amplitudes for static eccentricity and symmetry, respectively, taken from the spectrum presented in Figure 6—the case with 77% static eccentricity.

The indices $EALI_{stat}$ and $ESALI_{stat}$, calculated on the basis of the harmonic amplitudes in Tables 1 and 2 of the motor spectrums with 77% static eccentricity, are 0.2951 and 0.1477, respectively.

Table 1. The frequencies and amplitudes of the harmonics assigned to the static eccentricity measured in the motor spectrum with 77% static eccentricity.

Formula	Frequency [Hz]	Amplitude [dB]
$f_0 + 28f_r$	726.7	25.11
$ f_0 - 56f_r $	1303.3	28.96
$f_0 + 112f_r$	2756.7	30.66
$ f_0 - 140f_r $	3333.4	26.86
$f_0 + 196f_r$	4786.7	24.25

Table 2. The frequencies and amplitudes of the harmonics assigned to the symmetry measured in the motor spectrum with a static eccentricity of 77%.

Formula	Frequency [Hz]	Amplitude [dB]
$-f_0 + 28f_r$	627.7	76.46
$ -f_0 - 56f_r $	1403.3	61.88
$ f_0 - 84f_r $	1980	48.34
$f_0 + 84f_r$	2080	51.11
$-f_0 + 112f_r$	2656.7	60.24
$ -f_0 - 140f_r $	3433.4	56.13
$ f_0 - 168f_r $	4010	33.48
$f_0 + 168f_r$	4110	39.22
$-f_0 + 196f_r$	4686.7	33.56

Based on the Formulas (6) and (7) presented in Section 2, eccentricity indices were calculated for all obtained spectra from simulation and then placed in Table 3.

Table 3. List of eccentricity indices for various motor states calculated on the basis of results from FEM tests.

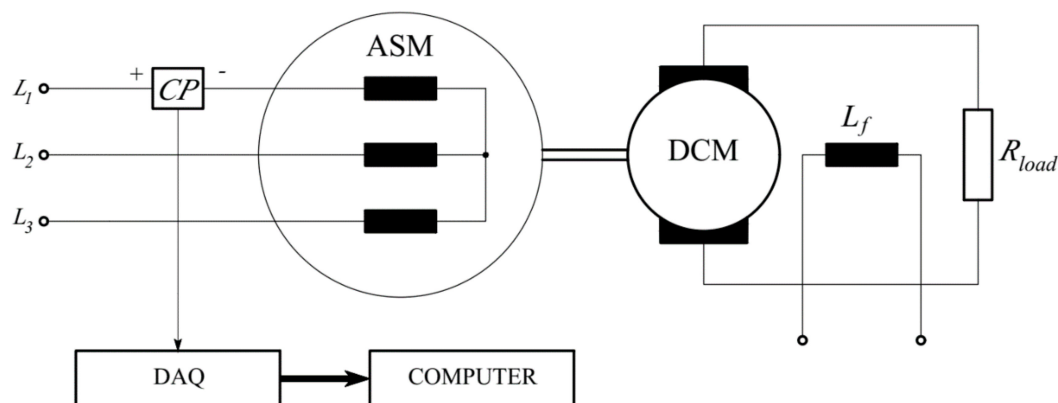
Motor Condition	<i>EALIstat</i>	<i>ESALIstat</i>	<i>EALIdyn</i>	<i>ESALIdyn</i>	<i>EALImix</i>	<i>ESALImix</i>
healthy	0	0	0.4427	0.0674	0.3168	0.0729
ecc. static	0.2951	0.1477	1.6180	0.4697	1.5650	0.2399
ecc. dynamic	0.1134	0.0289	1.3070	0.3730	0.5226	0.1042
ecc. mixed	0.1800	0.073	0.6655	0.1490	0.6332	0.2387

The summary of the results presented in Table 3 shows that the indices increase due to eccentricity. It is especially noticeable for indicators of dynamic and mixed eccentricity. Due to the fact that the skew of the rotor is not considered in the field model, the harmonics assigned to symmetry have high amplitudes; therefore, all the calculated indicators have low values.

4. Laboratory Test

4.1. Laboratory Stand

Laboratory tests were carried out on a modified Sg112M-4 motor. Previously, field-circuit calculations were made for this structure. The tested motor was loaded with a separately excited generator PZM5545 of rated data: $P_N = 4.5$ kW, $U_N = 230$ V, $I_N = 19.6$ A, $n_N = 1450$ rpm, $I_{fN} = 0.86$ A, resistively loaded. The schematic diagram of the system connections is shown in Figure 9.

**Figure 9.** Measurement circuits of motor where: *ASM*—cage induction motor, *CP*—current probe, *DCM*—DC generator, R_{load} —resistor, L_f —excitation winding inductance, *DAQ*—measurement card.

4.2. The Results of Laboratory Measurements

Measurements were carried out for four cases of motor condition:

- (a) symmetrical,
- (b) with a static eccentricity of 40%,
- (c) with a dynamic eccentricity of 40%,
- (d) with mixed eccentricity (dynamic 30% and static 40%).

At a star connection of the windings, the motor was supplied with phase-to-phase voltage with 400 volts effective value. All tests were carried out for the same stator, while only the rotors were replaced.

In the case of testing the motor with dynamic eccentricity, a rotor was mounted on eccentric bearings, while for the motor with static eccentricity, the rotor was mounted on specially grooved bearing plates. In the case of mixed eccentricity, both modifications were used.

In order to measure and record the current waveforms, the Tektronix A622-type transducers were used. The input signals were applied to analog inputs of the National Instruments BNC 6259 measurement card. The recording time of each measurement was set to 20 s with a sampling rate of 51,282 kS/s. In all cases, the motor was loaded so that the effective value of the stator current was 4 amps.

Recorded current waveforms were subjected to FFT frequency analysis. Based on the formulas for the characteristic frequencies (2)–(5), the harmonics indicating a given type of failure were searched and marked in Figures 10–13.

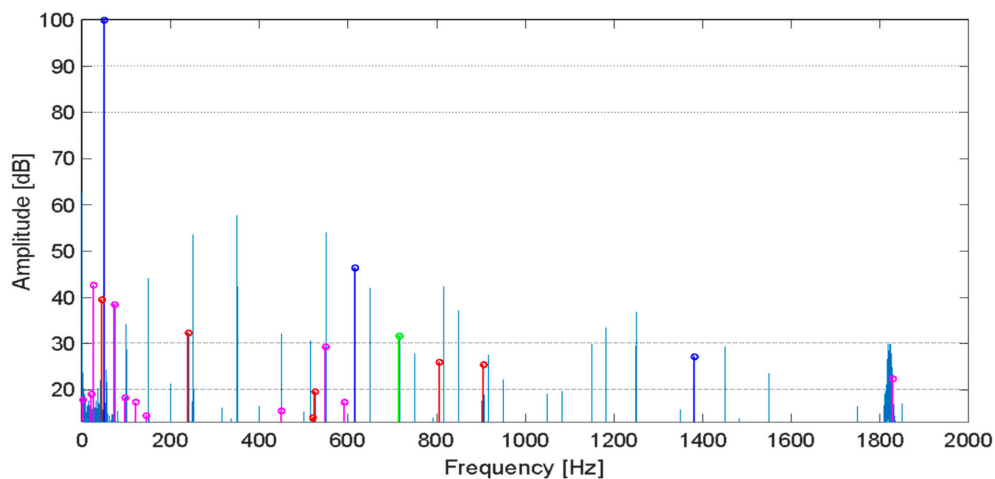


Figure 10. Spectrum of the stator current of a symmetrical motor.

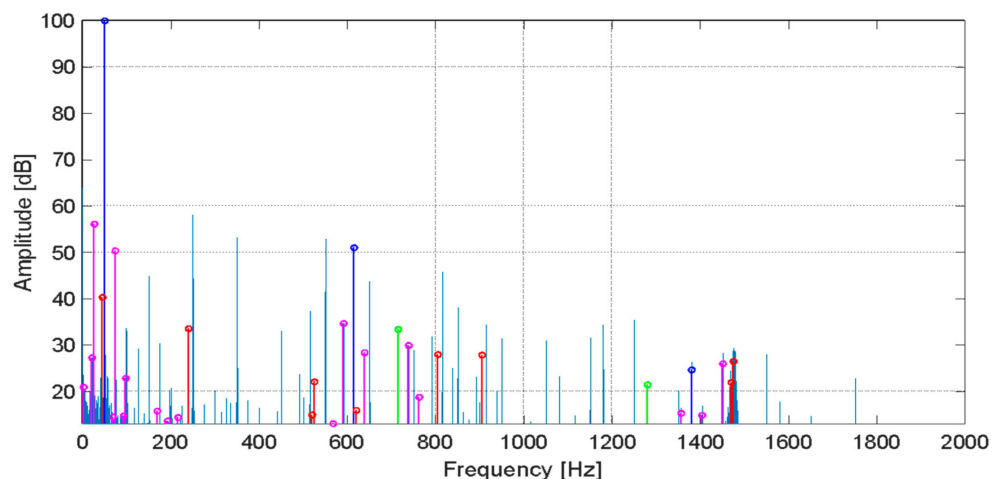


Figure 11. Spectrum of the stator current of a motor with 40% static eccentricity.

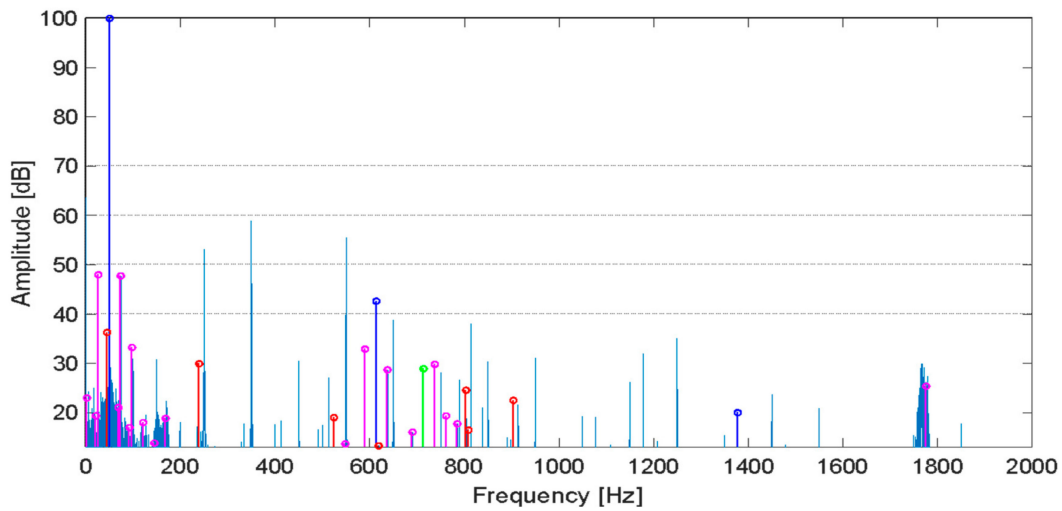


Figure 12. Spectrum of the stator current of a motor with 40% dynamic eccentricity.

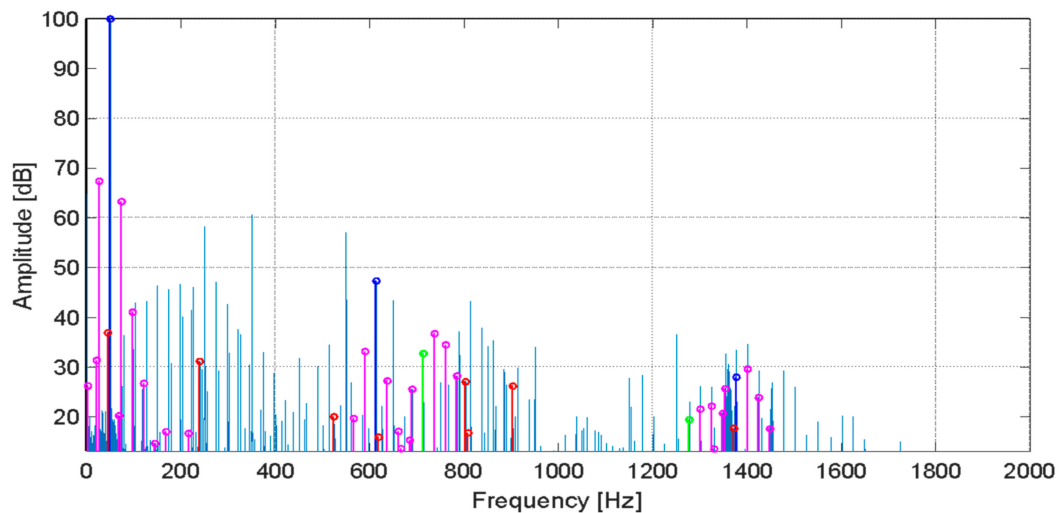


Figure 13. Spectrum of the stator current of a motor with 40% static eccentricity and 30% dynamic eccentricity.

For example, Tables 4 and 5 present the harmonic amplitudes appropriate for static eccentricity and symmetry, respectively, selected from the spectrum presented in Figure 11—the case with 40% static eccentricity.

Table 4. Frequencies and amplitudes of harmonics assigned to the static eccentricity, selected from the spectrum of the motor with 40% static eccentricity.

Formula	Frequency [Hz]	Amplitude [dB]
$f_0 + 28f_r$	715.2	33.37
$ f_0 - 56f_r $	1280.3	21.44

Table 5. Frequencies and amplitudes of harmonics assigned to the symmetry, selected from the spectrum of the motor with 40% static eccentricity.

Formula	Frequency [Hz]	Amplitude [dB]
$-f_0 + 28f_r$	615.2	51.01
$ -f_0 - 56f_r $	1380.3	24.66

The indices $EALI_{stat}$ and $ESALI_{stat}$ calculated on the basis of the harmonic amplitudes in Tables 4 and 5 of the motor spectrums with 40% static eccentricity are, respectively, 0.7243 and 0.4901.

On the basis of Formulas (8) and (9), the eccentricity indicators for each spectrum obtained from laboratory tests were calculated and then placed in Table 6. As in the case of field calculations, indicators increase as the degrees of eccentricity increase.

Table 6. List of eccentricity indicators for various motor states, calculated on the basis of laboratory test results.

Motor Condition	$EALI_{stat}$	$ESALI_{stat}$	$EALIdyn$	$ESALIdyn$	$EALImix$	$ESALImix$
Healthy	0.4299	0.3460	2.1303	1.5571	3.7572	2.4209
Static ecc.	0.7243	0.4901	3.0522	2.0097	5.8636	4.0987
Dynamic ecc.	0.4617	0.3770	2.7768	1.9255	7.2859	5.8287
Mixed ecc.	0.6923	0.4790	2.5454	1.6534	10.1277	8.2263

5. Examples of Motor Measurements in Industry

In order to obtain current signals for diagnostic purposes, the motors are measured directly, depending on the needs and possibilities, by installing measuring transducers (e.g., Rogowski coils) on the stator supply lines (Figure 14), at the output of the inverter (Figure 15) or by using secondary and protection circuits in the switchroom (Figures 16 and 17); this applies to the HV machines. On the other hand, the diagnostic signal in the form of an axial flux can be obtained using a measuring coil located on the non-driving side of the motor (Figure 18); this applies to both LV (low-voltage) and HV (high-voltage) machines.



Figure 14. Direct measurement of the motor phase currents with use of Rogowski coils.



Figure 15. Direct measurement of one phase current at the output of the inverter.



Figure 16. Measurement of current signals from secondary circuits in the switchroom.



Figure 17. Current and voltage probes clamped on protection circuits in the switchroom.



Figure 18. Flux measurement coil located on the non-driving side of the motor.

5.1. Diagnostic Measurements and Diagnosis of Eccentricity Levels—Motor 1

5.1.1. Condensate Extraction Pump Motor

The condensate extraction pumps are commonly installed in combined heat and power plants for pumping liquid originating from the condensation of steam and water vapor. Heat of condensation is used for heating in inside and outside installations while the condensate is traveling back to the steam boiler via heat exchangers. In every power block there are 2–3 pumps driven by HV motors. Once a year, advanced diagnostic measurements of the cage condition and rotor eccentricity are carried out. Based on diagnostic tests performed in 2012 and 2015, the eccentricity indicators were obtained and collected in Tables 7–9. Detailed illustrations with a selection of the characteristic

components of the current spectra are shown in Figures 19–25. Motor 1 basic data: 250 kW, 6 kV, 1487 rpm, 28.9 A.

5.1.2. Measurements in 2012 and 2015

In order to carry out the measurement, the transducers (current probes) are clamped around the wires in the secondary circuits of the motor phases. Measurement signals containing current waveforms in secondary circuits are recorded and then processed by appropriate software, resulting in amplitude–frequency spectra, among others. Based on the starting currents waveforms and the spectrum, machine diagnostics are performed.

The measurement results of Motor 1 are presented here. Looking at the spectra of this motor made on the basis of measurements distant in time, it is difficult to determine to what extent their changes, if noticeable, have an influence on the increase or decrease of the level of eccentricity and, consequently, on further operation of the drive. Whereas the use of even two of the simplest indicators answers the question.

5.1.3. Comparison of Spectra and Indicators for Static Eccentricity

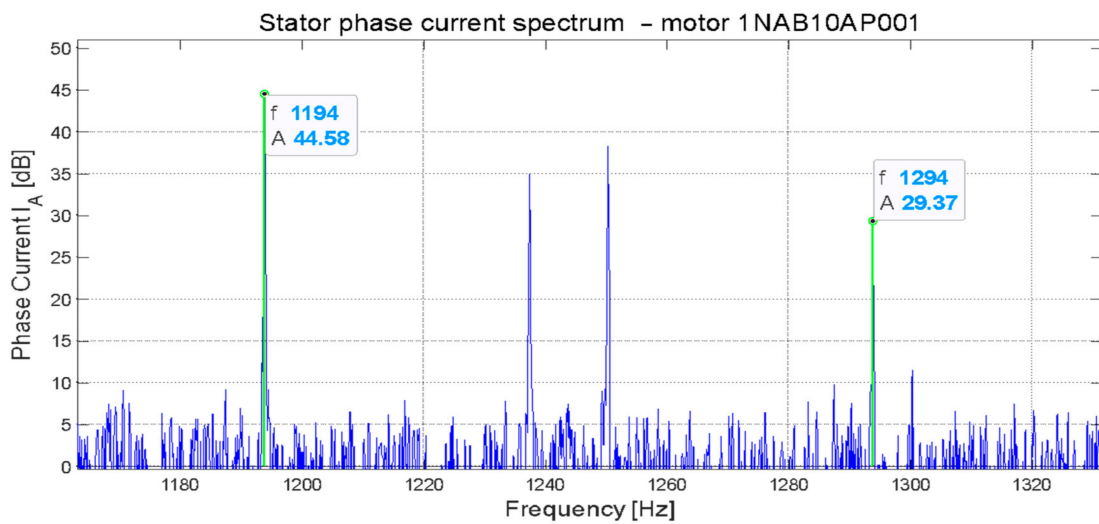


Figure 19. Spectrum components specific to static eccentricity—measurement in 2012.

Principal slot harmonics Psh : 2338 Hz/39.64 dB and 4625 Hz/26.24 dB.

Indicators for static eccentricity—measurement in 2012: $EALI_{stat} = 1.21$, $ESALI_{stat} = 1.47$.

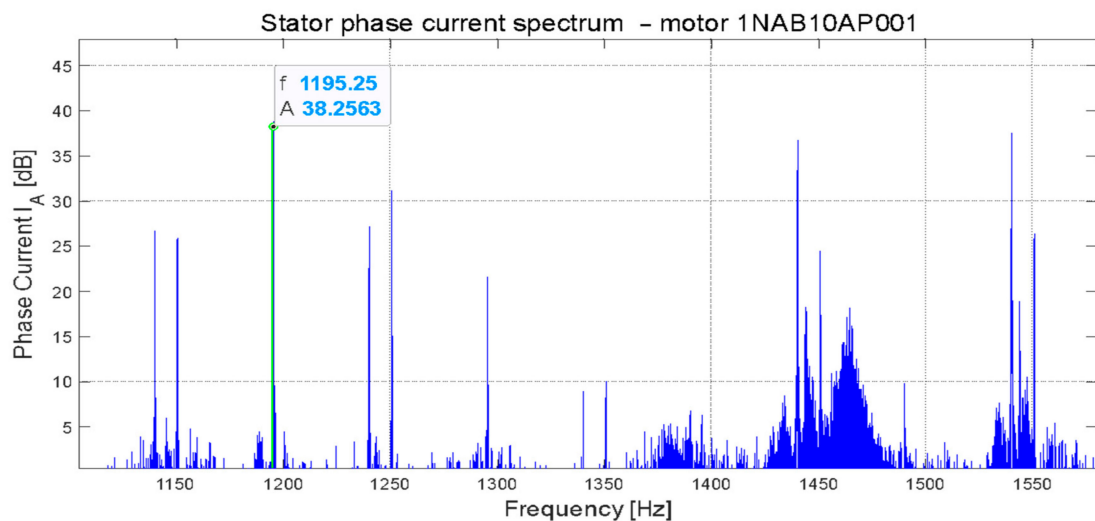


Figure 20. Spectrum components specific to static eccentricity—measurement in 2015.

Principal slot harmonics Psh : 2341 Hz/27.36 dB and 4631 Hz/14.05 dB.

Indicators for static eccentricity—measurement in 2015: $EALI_{stat} = 1.25$, $ESALI_{stat} = 1.58$.

Table 7. Static eccentricity indicators comparison.

Year	$EALI_{stat}$ [dB]	$ESALI_{stat}$ [dB]
2012	1.21	1.47
2015	1.25	1.58

Recommendation: The comparison shows a slight increase in both indicators during the 3-year period, indicating some minimal development of static eccentricity.

5.1.4. Comparison of Spectra and Indicators for Dynamic Eccentricity

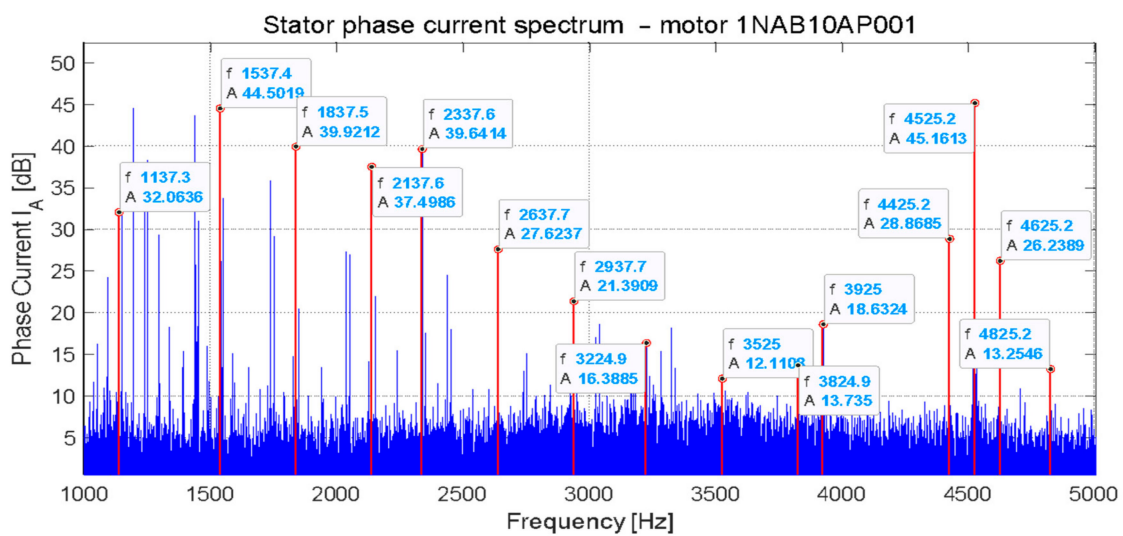


Figure 21. Spectrum components specific to dynamic eccentricity—measurement in 2012.

Indicators for dynamic eccentricity—measurement in 2012: $EALI_{dyn} = 5.33$, $ESALI_{dyn} = 4.97$.

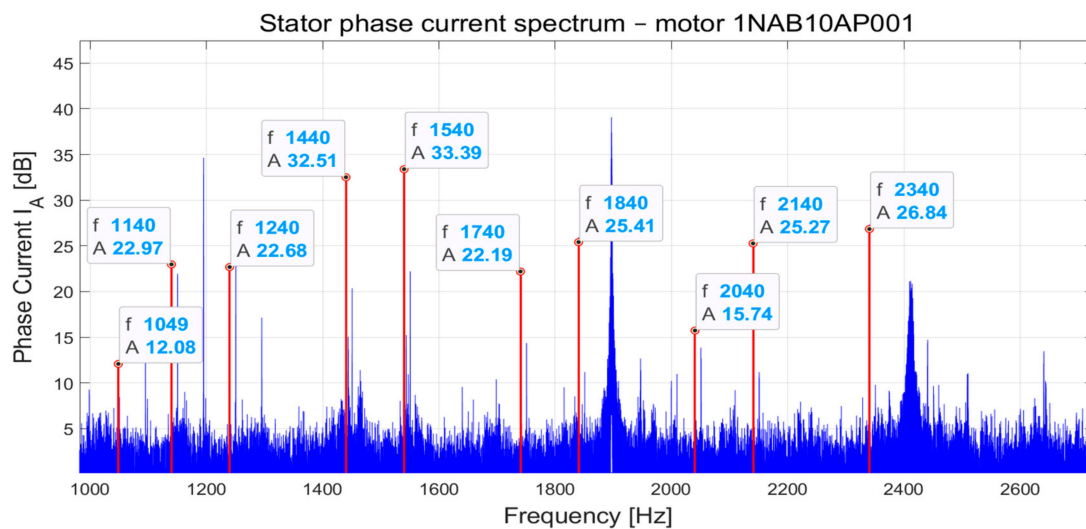


Figure 22. Spectrum components specific to dynamic eccentricity—measurement in 2015.

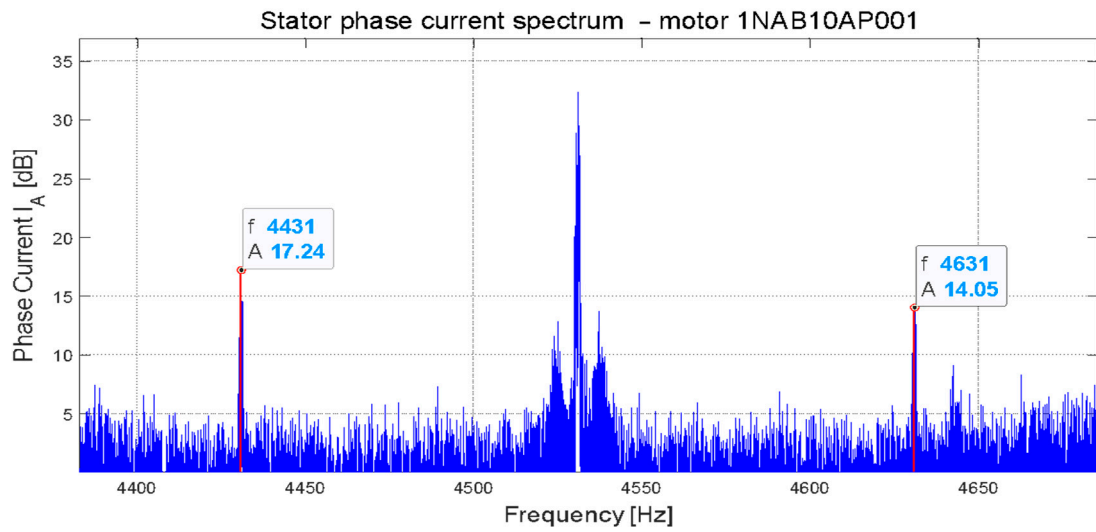


Figure 23. Spectrum components specific to dynamic eccentricity—measurement in 2015, range 4400–4600 Hz.

Indicators for dynamic eccentricity—measurement in 2015: $EALI_{dyn} = 8.61$, $ESALI_{dyn} = 9.91$.

Table 8. Dynamic eccentricity indicators comparison.

Year	$EALI_{dyn}$ [dB]	$ESALI_{dyn}$ [dB]
2012	5.33	4.97
2015	8.61	9.91

Recommendation: The comparison shows a clear, significant increase in both indicators over the 3-year period, indicating the development of dynamic eccentricity.

5.1.5. Comparison of Spectra and Indicators for Mixed Eccentricity

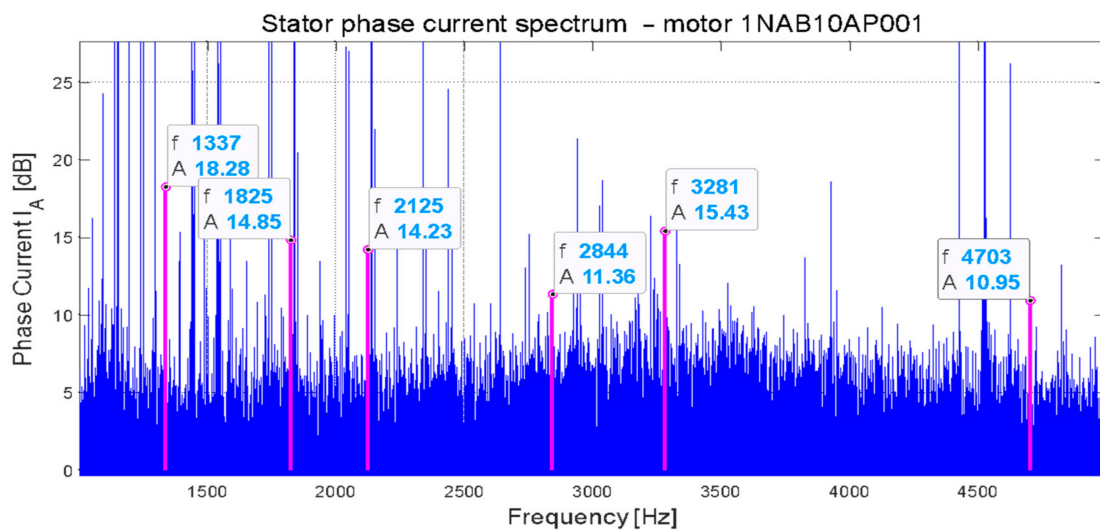


Figure 24. Spectrum components specific to mixed eccentricity—measurement in 2012.

Indicators for mixed eccentricity—measurement in 2012: $EALI_{mix} = 1.40$, $ESALI_{mix} = 0.54$.

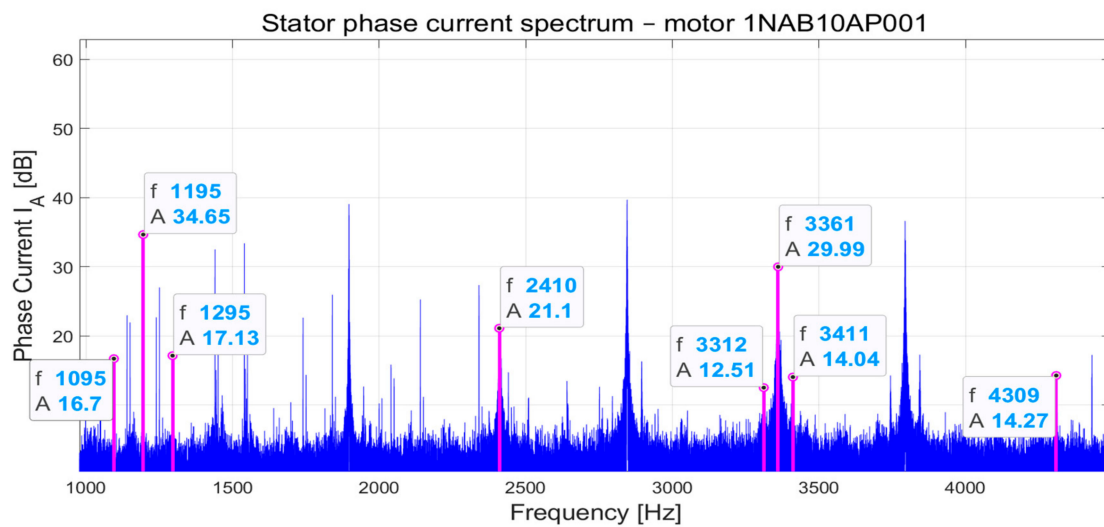


Figure 25. Spectrum components specific to mixed eccentricity—measurement in 2015.

Indicators for mixed eccentricity—measurement in 2015: $EALI_{mix} = 2.70$, $ESALI_{mix} = 2.40$.

Table 9. Mixed eccentricity indicators comparison.

Year	$EALI_{mix}$ [dB]	$ESALI_{mix}$ [dB]
2012	1.40	0.54
2015	2.70	2.40

Recommendation: The comparison shows a visible, significant increase in both indicators over a period of 3 years, indicating the development of mixed eccentricity.

5.2. Diagnostic Measurements and Diagnosis of Eccentricity Levels—Motor 2

In any power plant that produces electricity using steam turbines, the most important machines in the individual power blocks are the feed water pumps for steam production. The motors that drive the feed water pumps are the most powerful and of the most importance. Usually there are two of them in each block: one running and the other in reserve. Sudden failure of such a machine means that within a few seconds the same spare machine must be switched on to the operation or the block will be out of service.

Once a year, advanced diagnostic measurements of the cage condition, rotor eccentricity, noise and mechanical vibrations are carried out using the non-invasive method mentioned in Section 5.1 above. Based on diagnostic tests performed in 2014 and 2015, the eccentricity indicators were obtained and collected in Tables 10–12. Feedwater pump Motor 2 data: 3500 kW, 6 kV, 1491 rpm, 390 A. Measurements was made in 2014 and 2015. Detailed illustrations with a selection of the characteristic components of the current spectra are shown in Figures 26–32.

5.2.1. Comparison of Spectra and Indicators for Static Eccentricity

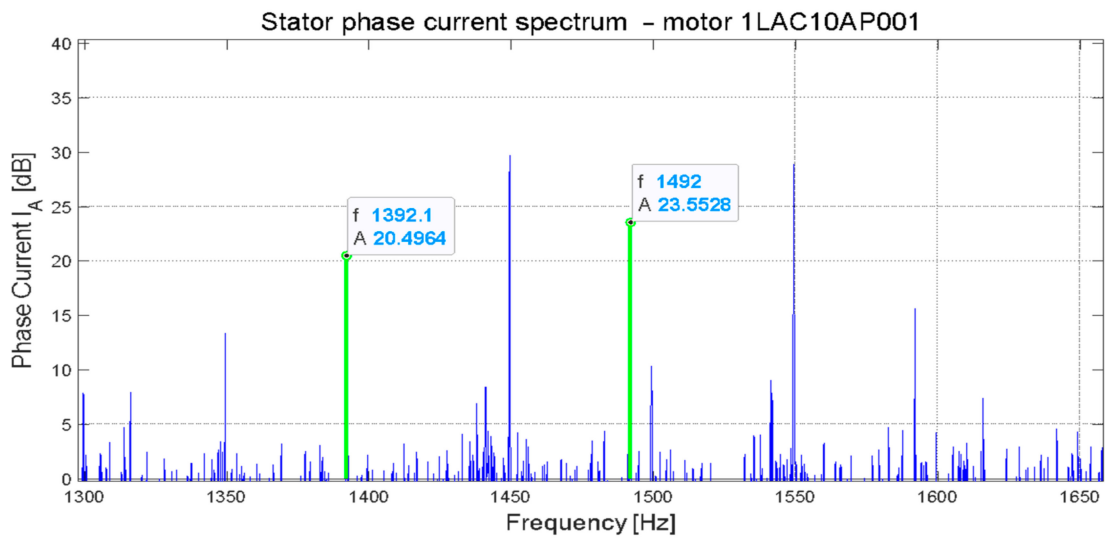


Figure 26. Spectrum components specific to static eccentricity—measurement in 2014.

Principal slot harmonics Psh : 2934 Hz/17.2 dB and 3034 Hz/19.43 dB.

Indicators for static eccentricity—measurement in 2014: $EALI_{stat} = 1.20$, $ESALI_{stat} = 1.45$.

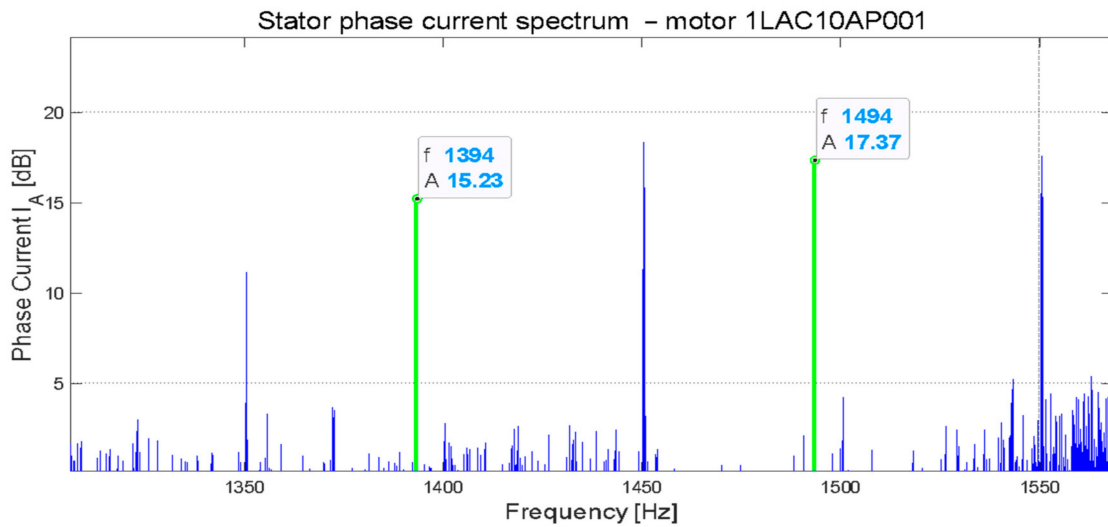


Figure 27. Spectrum components specific to static eccentricity—measurement in 2015.

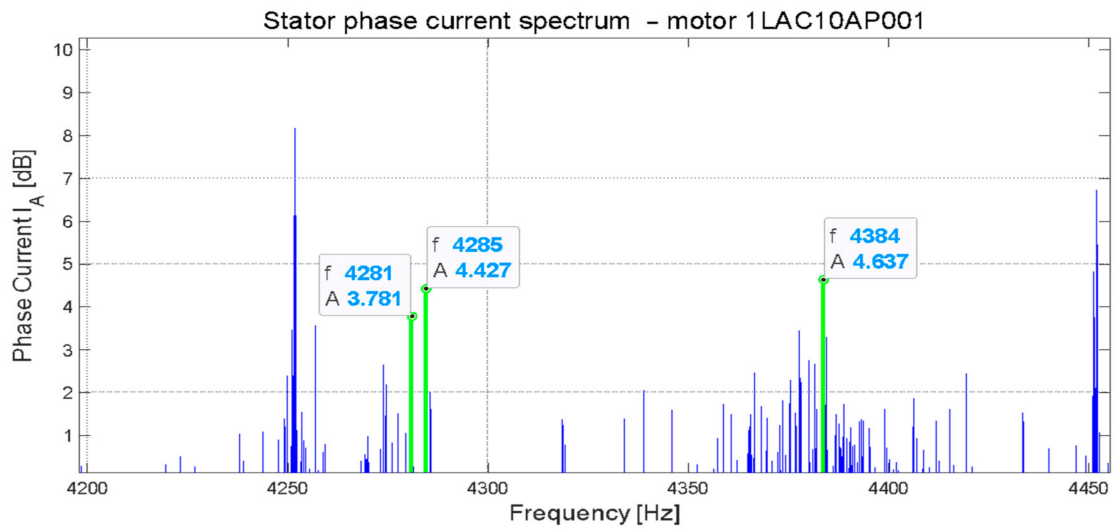


Figure 28. Spectrum components specific to static eccentricity—measurement in 2015, range 4200–4440 Hz.

Principal slot harmonics Psh : 2937 Hz/10.55 dB and 3037 Hz/12.02 dB.

Indicators for static eccentricity—measurement in 2015: $EALI_{stat} = 1.82$, $ESALI_{stat} = 2.22$.

Table 10. Static eccentricity indicators comparison.

Year	$EALI_{stat}$ [dB]	$ESALI_{stat}$ [dB]
2014	1.20	1.45
2015	1.82	2.22

Recommendation: The comparison shows a small but clear increase in both indicators over a 1-year period, indicating some minimal development of static eccentricity.

5.2.2. Comparison of Spectra and Indicators for Dynamic Eccentricity

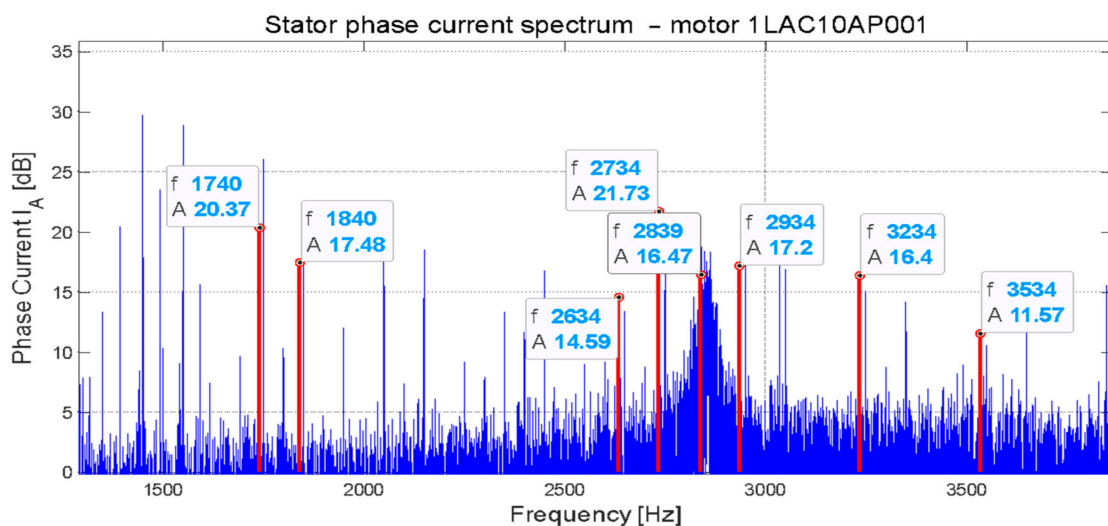


Figure 29. Spectrum components specific to dynamic eccentricity—measurement in 2014.

Indicators for dynamic eccentricity—measurement in 2014: $EALI_{dyn} = 3.24$, $ESALI_{dyn} = 3.10$.

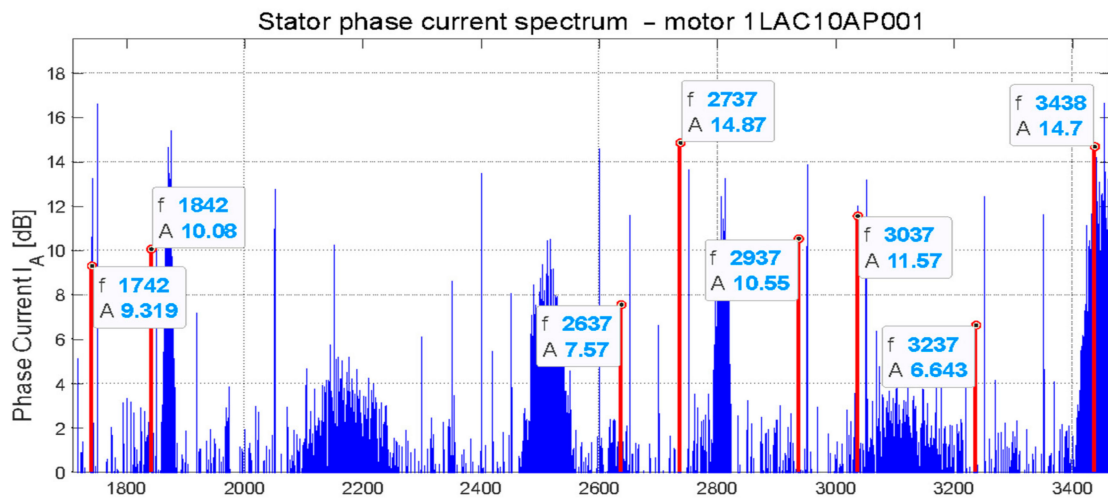


Figure 30. Spectrum components specific to dynamic eccentricity—measurement in 2015.

Indicators for dynamic eccentricity—measurement in 2015: $EALI_{dyn} = 2.68$, $ESALI_{dyn} = 3.10$.

Table 11. Dynamic eccentricity indicators comparison.

Year	$EALI_{dyn}$ [dB]	$ESALI_{dyn}$ [dB]
2014	3.34	3.10
2015	2.68	3.10

Recommendation: The comparison shows a slight decrease in both indicators over the year, indicating the same or slightly smaller, but still significant level of dynamic eccentricity.

5.2.3. Comparison of Spectra and Indicators for Mixed Eccentricity

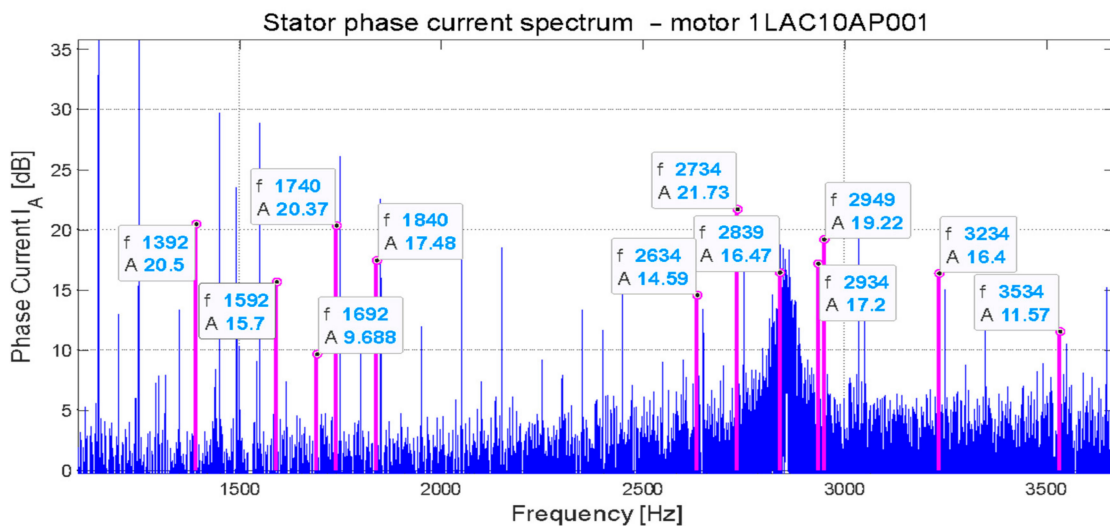


Figure 31. Spectrum components specific to mixed eccentricity—measurement in 2014.

5.2.4. Comparison of Spectra and Indicators for Mixed Eccentricity

Indicators for mixed eccentricity—measurement in 2014: $EALI_{mix} = 4.50$, $ESALI_{mix} = 4.23$.

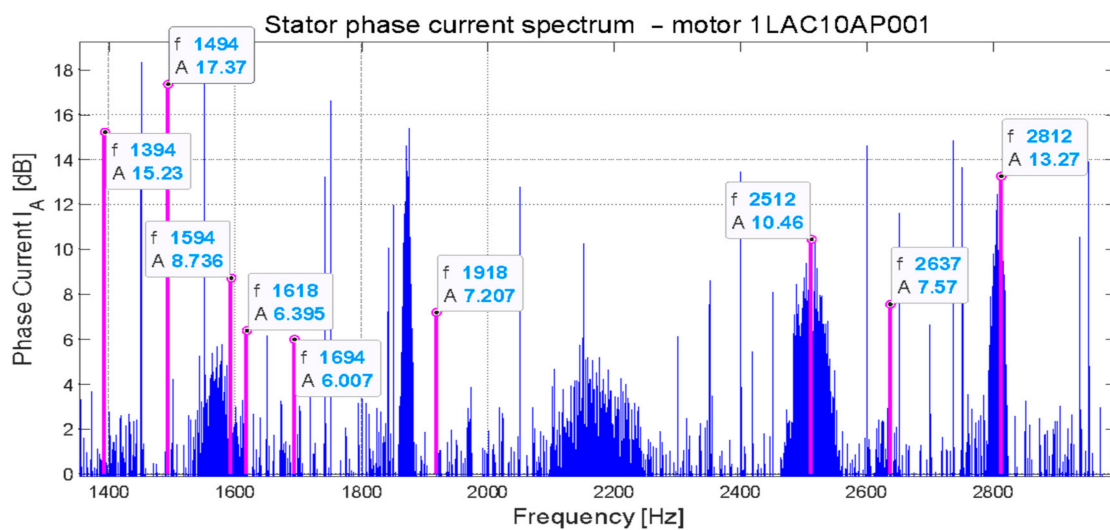


Figure 32. Spectrum components specific to mixed eccentricity—measurement in 2015.

Indicators for mixed eccentricity—measurement in 2015: $EALI_{mix} = 2.30$, $ESALI_{mix} = 1.90$.

Table 12. Mixed eccentricity indicators comparison.

Year	$EALI_{mix}$ [dB]	$ESALI_{mix}$ [dB]
2014	4.50	4.23
2015	2.30	1.90

Recommendation: The comparison shows a significant decrease in both indicators over the year, indicating a much lower level of mixed eccentricity, which, combined with a slight decrease in dynamic eccentricity, will significantly reduce vibration levels and relieve bearings. This is the result of service activities.

5.3. Diagnostic Measurements and Diagnosis of Eccentricity Levels—Motor 3

5.3.1. Extruder Installation Motor

The squirrel cage Motor 3 in an extruder installation worked in a continuous operation regime. The start of the motor was carried out by initial acceleration with use of a lower power external motor in order to eliminate the danger of significant starting currents and overheating. Monitoring of Motor 3 provided by the owner was limited to checking the temperature of the windings and the level of mechanical vibrations of the bearings. Once a year, advanced diagnostic measurements of the cage condition, rotor eccentricity, level of partial discharges, noise and mechanical vibrations were carried out.

In order to carry out the measurement, the transducers (current probes) are clamped around the wires in the secondary circuits of the motor phases. Measurement signals containing current waveforms in secondary circuits are recorded and then processed by appropriate software, resulting in amplitude–frequency spectra, among others. Based on the starting currents waveforms and the spectrum, machines rotor and eccentricity diagnoses are performed.

To check the level and nature of partial discharges, the Rogowski coils must be clamped around each phase cable of the machine supply. The signals from each phase are recorded and after processing the recommendation can be completed.

The machine has not been repaired for 5 years; it was only the increase in the vibration level of the bearings and PD level that prompted the operator to remove the machine from operation and repair it, including the stator windings and replacement of the bearings. Based on year-by-year diagnostic tests, the eccentricity indicators were obtained and collected in Table 13. Extruder basic motor data: 1640 kW, 6 kV, 1485 rpm, 182.6 A.

5.3.2. Comparison of EALI Indicators for Dynamic and Mixed Eccentricity over the Years 2015–2019

Table 13. Summary of dynamic and mixed eccentricity indicators for Motor 3.

Year	$EALI_{dyn}$ [dB]	$EALI_{mix}$ [dB]
2015	4.289	18.508
2016	5.809	19.077
2017	6.417	23.726
2018	9.205	30.662
2019	4.425	16.735

6. Discussion

The use of the described method for evaluation levels of induction motors' eccentricity does not require any additional procedures apart from those that are performed with standard diagnostic tests, such as measurement and processing of current signals or axial flux in order to diagnose the rotor winding. It can therefore be said that the data needed to assess eccentricity are available, as if by the way.

Although the methods for stator current and axial flux diagnostic signals acquisition are identical for diagnosing both cage condition and eccentricity, the ranges of use for these two diagnoses differ substantially. The values of the aforementioned RFI factors define the range of the cage failure for all induction machines, regardless of their size, number of pole pairs, type, type of work, LV or HV power supply, etc. Thousands of machines were tested for this purpose. On the other hand, the values of the coefficients determining the degree of eccentricity refer only to a single, individual machine, at least so far. Perhaps the values of the eccentricity indices would be similar for a given type of machine with similar symptoms. However, in order to possibly standardize the criteria, a significant number of machines of each type would have to be tested. It is definitely the right path, but it requires a lot of work and time.

The method based on the use of the above indicators has been verified by the model, laboratory tests and measurements in industry at machine work places.

Any changes in the form of bearing wear, alignment deterioration or deteriorating load impact on the motor will be reflected in the current and axial flux waveforms, and, as a result, in the increase of indicators obtained based on the spectra.

Systematic observation of indicators from time to time may provide the operator with information about the condition of the machine and an inspiration for possible service procedures.

7. Conclusions

Bearing wear or defect, or imbalance or defect in the rotor cage is reflected in the change in the appearances of the current and axial flux spectra, but on the basis of visual impression it is difficult to determine to what extent this change may affect the level of eccentricity and the operation of the machine.

The use of coefficients–numerical indicators enabled quantitative determination of eccentricity levels of induction motors.

It needs to be highlighted that to obtain the eccentricity indices, the same measurement data are used for the diagnosis of the rotor condition. The result of the motor test on the basis of the current or axial flux spectrum in terms of the rotor winding condition is obtained immediately, while the eccentricity index is only used for comparison with the next test. However, after a few measurements taken, separated in time, the trend is clearly visible and a maintenance crew can keep an eye on the machine to correct, for example, the alignment of the motor with the load machine at the right moment, or to plan the replacement of bearings. This method seems to be effective and useful, as shown by the authors' experience.

The case of the 1640 kW, 6 kV motor in the extruder installation, which worked for 5 years without replacing the bearings and was measured every year in 2015–2019, confirms the usefulness of the method. Over the next 4 years, the level of bearing vibrations systematically increased, and with it the indicators of the eccentricity level (Table 13, Figure 33). After replacing the bearings in 2019, the indicators decreased significantly. This case, and many others, illustrates well the sense of using eccentricity indicators.

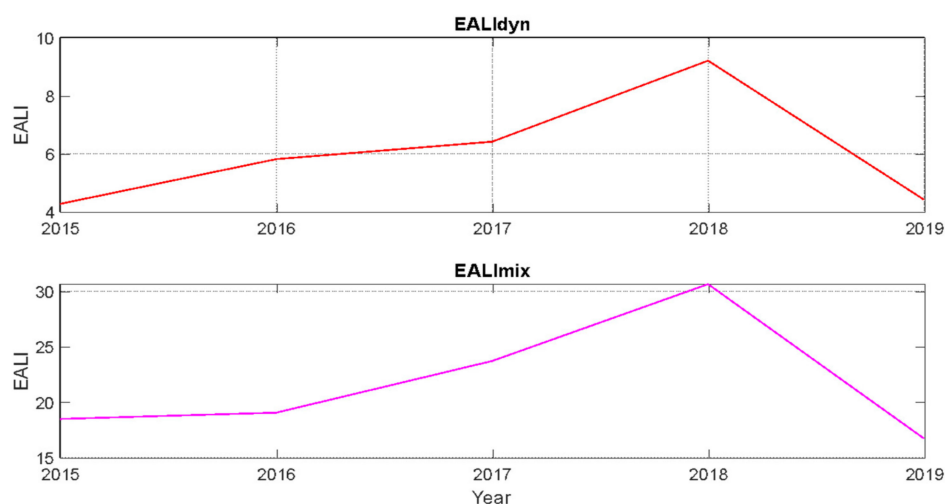


Figure 33. Changes of Eccentricity Amplitude Level Index (EALI) indicators for dynamic and mixed eccentricity over the years 2015–2019. In 2019, the machine was overhauled. Among other things, bearings were replaced.

It has been shown, among other things, that over time during motor operation the degree of eccentricity may increase, especially if the machine is not serviced; while if it is supervised and properly serviced, the degree of eccentricity significantly decreases. Furthermore, several examples from measurements in industry and laboratory show the increase in these indicators due to the increase in the degree of eccentricity.

The application of the method enables detection of changes in machine operation and determination of their trend as well as comparison with levels of measured mechanical vibrations.

Author Contributions: Conceptualization, J.P., A.D. and M.S.; methodology, J.P., M.S. and A.D.; software, A.D. and M.S.; validation, J.P., A.D. and M.S.; formal analysis, J.P., M.S. and A.D.; investigation, A.D. and M.S.; resources, A.D. and M.S.; data curation, J.P., A.D. and M.S.; writing—original draft preparation, J.P. and M.S.; writing—review and editing, J.P., M.S. and A.D.; visualization, A.D.; supervision, J.P. and M.S. All authors have read and agreed to the published version of the manuscript.

Funding: This research, which was carried out under the theme Department of Electrical Engineering E-2, was founded by the subsidies on science granted by the Polish Ministry of Science and Higher Education.

Institutional Review Board Statement: Not applicable.

Informed Consent Statement: Not applicable.

Conflicts of Interest: The authors declare no conflict of interest.

Abbreviations

$A_{eccType}$	harmonic amplitudes for a given type of eccentricity
A_{sym}	amplitude of the basic slot harmonic (Psh) appropriate for magnetic symmetry
d_r	vector of the current displacement of the rotor axis in relation to the stator axis
d_s	vector of constant displacement of the rotor axis in relation to the stator axis
δ_0	an average air gap length considering the slot opening geometry and the Carter's factor of a healthy motor,
$EALI$	Eccentricity Amplitude Level Index
$eccType$	a kind of eccentricity: static— <i>stat</i> , dynamic— <i>dyn</i> , mixed— <i>mix</i>
$ESALI$	Eccentricity Square Amplitude Level Index
ε_s	level of static eccentricity
ε_d	level of dynamic eccentricity
f_0	mains voltage frequency
f_{dyn}	frequency of the stator current or flux spectrum components specific to dynamic eccentricity
f_{mix}	frequency of the stator current or flux spectrum components specific to mixed eccentricity
f_r	rotating frequency
f_{stat}	frequency of the stator current or flux spectrum components specific to static eccentricity
f_{sym}	frequency of the stator current or flux spectrum components specific to the machine's magnetic symmetry
g	number associated with N and p , ranging from 1 to $2p$ depending on the magnetic couplings of the stator and rotor windings
N	number of rotor slots
n	rotor speed
N_s	number of stator slots
p	number of pole pairs
Psh	Principal slot harmonics
T_b	critical (maximum) torque
T_{bn}	critical nominal torque

References

- Weinreb, K. Diagnostics of an Induction Motor Rotor by the Spectral Analysis of Stator Currents. *Ther. Eng.* **2013**, *60*, 1006–1023. [CrossRef]
- Weinreb, K.; Petryna, J. Metoda wykrywania ekscentryczności wirnika w maszynach indukcyjnych. *Masz. Elektr. Zesz. Probl.* **1998**, *55*, 123–128.
- Petryna, J.; Guziec, K.; Weinreb, K. Bezinwazyjne diagnozowanie on-line maszyn i napędów prądu przemiennego w warunkach zagrożenia wybuchem. In Proceedings of the Materiały IV Seminarium Technicznego BOBRME KOMEL "Problemy Eksploatacji Górniczych Napędów Dołowych", Ustroń, Poland, 5–6 November 1998.
- Petryna, J. Diagnostyczna baza danych napędów elektrycznych w energetyce dla potrzeb remontowych. In Proceedings of the Materiały IV Konferencji Naukowo-Technicznej Problemy i Innowacje w Remontach Energetycznych, Łądek-Zdrój, Poland, 28–30 November 2001.
- Petryna, J.; Sułowicz, M.; Duda, A.; Guziec, K. Możliwości wykorzystania strumienia unipolarnego w diagnostyce maszyn prądu przemiennego. *Napędy Sterow.* **2014**, *16*, 100–105.
- Weinreb, K.; Sułowicz, M. Skuteczne wykrywanie ekscentryczności dynamicznej w silniku asynchronicznym. *Masz. Elektr. Zesz. Probl.* **2009**, *83*, 207–212.
- Szymaniec, S. Diagnostyka eksploatacyjna uszkodzeń napędów elektrycznych w przemyśle. *Napędy Sterow.* **2011**, *13*, 84–89.
- Bellini, A.; Filipetti, F.; Tassoni, C.; Capolino, G.A. Advances in Diagnostic Techniques for Induction Machines. *IEEE Trans. Ind. Electron.* **2008**, *55*, 4109–4126. [CrossRef]
- Thomson, W.T.; Fenger, M. Current signature analysis to detect induction motor faults. *IEEE Ind. Appl. Mag.* **2001**, *7*, 26–34. [CrossRef]
- Fenger, M.; Lloyd, B.A.; Thomson, W.T. Development of a tool to detect faults in induction motors via current signature analysis. In Proceedings of the IEEE-IAS/PCA Cement Industry Technical Conference, Dallas, TX, USA, 4–9 May 2003; pp. 37–46. [CrossRef]
- Miljković, D. Brief Review of Motor Current Signature Analysis. *HDKBR INFO Mag.* **2015**, *5*, 14–26. Available online: <https://hrcak.srce.hr/148715> (accessed on 30 January 2021).
- Burriel-Valencia, J.; Puche-Panadero, R.; Martinez-Roman, J.; Sapena-Bano, A.; Pineda-Sanchez, M. Fault Diagnosis of Induction Machines in a Transient Regime Using Current Sensors with an Optimized Slepian Window. *Sensors* **2018**, *18*, 146. [CrossRef] [PubMed]
- Faiz, J.; Ebrahimi, B.M.; Toliyat, H.A. Effect of Magnetic Saturation on Static and Mixed Eccentricity Fault Diagnosis in Induction Motor. *IEEE Trans. Magn.* **2009**, *45*, 3137–3144. [CrossRef]
- Cusidó, J.; Romeral, L.; Ortega, J.A.; Garcia, A.; Riba, J. Signal Injection as a Fault Detection Technique. *Sensors* **2011**, *11*, 3356–3380. [CrossRef] [PubMed]
- Xu, X.; Han, Q.; Chu, F. Review of Electromagnetic Vibration in Electrical Machines. *Energies* **2018**, *11*, 1779. [CrossRef]
- Duda, A.; Drozdowski, P. Induction Motor Fault Diagnosis Based on Zero-Sequence Current Analysis. *Energies* **2020**, *13*, 6528. [CrossRef]

17. Gyftakis, K.N.; Kappatou, J.C. The Zero-Sequence Current as a Generalized Diagnostic Mean in Δ -Connected Three-Phase Induction Motors. *IEEE Trans. Energy Convers.* **2014**, *29*, 138–148. [[CrossRef](#)]
18. Gyftakis, K.N.; Kappatou, J.C. The zero-sequence current spectrum as an on-line static eccentricity diagnostic mean in Δ -connected PSH-induction motors. In Proceedings of the 2013 9th IEEE International Symposium on Diagnostics for Electric Machines, Power Electronics and Drives (SDEMPED), Valencia, Spain, 27–30 August 2013; pp. 302–308.
19. Duda, A.; Sułowicz, M. A New Effective Method of Induction Machine Condition Assessment Based on Zero-Sequence Voltage (ZSV) Symptoms. *Energies* **2020**, *13*, 3544. [[CrossRef](#)]
20. Constantin, A.; Fireteanu, V. Efficiency in the detection of three important faults in induction motors through external magnetic field. In Proceedings of the 2015 9th International Symposium on Advanced Topics in Electrical Engineering (ATEE), Bucharest, Romania, 7–9 May 2015; pp. 430–435.
21. Vitek, O.; Janda, M.; Hajek, V.; Bauer, P. Detection of eccentricity and bearings fault using stray flux monitoring. In Proceedings of the 8th IEEE Symposium on Diagnostics for Electrical Machines, Power Electronics & Drives, Bologna, Italy, 5–8 September 2011; pp. 456–461.
22. Gyftakis, K.N.; Panagiotou, P.A.; Lee, S.B. The Role of the Mechanical Speed Frequency on the Induction Motor Fault Detection via the Stray Flux. In Proceedings of the 2019 IEEE 12th International Symposium on Diagnostics for Electrical Machines, Power Electronics and Drives (SDEMPED), Toulouse, France, 27–30 August 2019; pp. 201–207.
23. Chernyavska, I.; Vitek, O. Analysis of air-gap eccentricity in inverter fed induction motor by means of motor current signature analysis and stray flux of motor. In Proceedings of the 2017 IEEE 11th International Symposium on Diagnostics for Electrical Machines, Power Electronics and Drives (SDEMPED), Tinos, Greece, 29 August–1 September 2017; pp. 72–76.
24. Gao, Z.; Liu, X. An Overview on Fault Diagnosis, Prognosis and Resilient Control for Wind Turbine Systems. *Processes* **2021**, *9*, 300. [[CrossRef](#)]
25. Aslam, M.; Bantan, R.A.R.; Khan, N. Monitoring the Process Based on Belief Statistic for Neutrosophic Gamma Distributed Product. *Processes* **2019**, *7*, 209. [[CrossRef](#)]
26. Sobczyk, T.J.; Drozdowski, P. Inductances of electrical machine winding with a nonuniform air-gap. *Arch. Elektrotechnik* **1993**, *76*, 213–218. [[CrossRef](#)]
27. Węgiel, T.; Weinreb, K.; Sułowicz, M. Main inductances of induction motor for diagnostically specialized mathematical models. *Arch. Electr. Eng.* **2010**, *59*, 51–66. [[CrossRef](#)]